XLI CILAMCE
XLI Ibero-Latin American Congress on Computational Methods in Engineering
16-19 November, 2020 FOZ DO IGUAÇU PARANÁ - BRAZIL

Dynamic analysis of soil-structure interaction problems using hexahedral finite elements with reduced integration

Michael. R. M. Visintainer[1], Alexandre L. Braun[1]

[1] *Programa de Pós-Graduação em Engenharia Civil (PPGEC), Universidade Federal do Rio Grande do Sul (UFRGS)*
Av. Osvaldo Aranha, 99- 3º andar, CEP 90035-190, Porto Alegre, RS, Brasil
michael.rene@ufrgs.br, alexandre.braun@ufrgs.br

Abstract. In the present work, a numerical simulation is performed to obtain the soil influence on the dynamic response of structures under cyclic loading. The spatial discretization of the soil and the structure is carried out here by employing hexahedral isoparametric elements with reduced integration and an efficient technique is employed for controlling the so-called hourglass modes. The load transfer between the soil and the structure is performed by a three-dimensional contact algorithm based on the penalty method formulation, where small interpenetrations can occur between the deformable bodies in contact. A corotational approach at element level is used to deal with physically and geometrically nonlinear analysis, where the physical nonlinearity is due to the elastoplastic behavior of the materials employed. Dynamic equilibrium equation is solved using the Newmark's method and the Generalized-α method. Numerical examples are performed and compared with predictions obtained by the software ANSYS in order to verify the present algorithm.

Keywords: dynamic analysis, soil-structure interaction, finite element method, reduced integration.

1 Introduction

The soil-structure interaction corresponds to the load transfer between foundation and soil through the contact between the two media, performing a fundamental role in the overall structure response. Studies presented by Chopra and Gutierrez [1] and Bielak [2] have already demonstrated that the dynamic response of structures resting on flexible soil shows a very different behavior when compared to the same structure resting on a rigid base. According to Novak and Hifnawi [3] and Menglin et al. [4], the main reason for this difference is that part of the vibrational energy of the structure on flexible soil is dissipated by the propagation of elastic waves in soil and by hysteretic losses in soil. More information on soil-structure models may be found in Dutta and Roy [5], while a review of soil-structure interaction is show in Kausel [6].

Note that three-dimensional dynamic analysis of soil-structure interaction based on the Finite Element Method (FEM) requires a high computational cost due to the inherent nonlinear nature of contact problems. An alternative to improve computational efficiency is the use of finite elements with reduced integration instead of finite elements with full quadrature. In this way, Hu and Nagy [7] presented a formulation for hexahedral elements with one-point quadrature that was later extended by Duarte Filho and Awruch [8] to geometrically nonlinear static and dynamic problems. Braun and Awruch [9] extended that formulation to dynamic problems in the nonlinear range employing the generalized-α method. Hexahedral elements with one-point quadrature in elastoplastic problems were studied by Schmidt [10], who adopted the optimized parameter proposed by Reese [11] in the element stability matrix. A similar formulation was later used by Braun and Awruch [12,13] in order to simulate the mechanical behavior of soils using the Modified Cam-Clay model.

Among most of the existing formulations to analyze contact problems numerically, the penalty and Lagrange multiplier methods are the most popular. In the penalty method, small interpenetrations are allowed between the elements in contact, where a penalty parameter is used to satisfy approximately the impenetrability restriction for bodies in contact. A finite element treatment for large deformation contact problems between

deformable bodies was presented by Laursen and Simo [14], where a convected coordinate system was settled in order to obtain a friction law with frame indifference. Chen et al. [15] proposed a formulation similar to Laursen and Simo [14] that evaluates the sliding term in the reference configuration in order to overcome the limitations found in the cases where the sliding extends over the boundary of adjacent elements, considering that the corresponding convected coordinate systems are locally defined and, therefore, discontinuous. More information on the correct numerical treatment of contact problems may be found in Wrigger [16] and Laursen [17].

Therefore, hexahedral elements with reduced integration and an efficient stabilization technique are used in this work to observe the behavior of a structure under cyclic loading resting on a soil layer. The load transfer between soil and structure is carried out using a three-dimensional contact formulation based on the penalty method. Physically and geometrically nonlinear analyses are performed using a corotational formulation. The finite element software ANSYS is employed to verify the present algorithm.

2 Finite element model

2.1 The principle of virtual work

The principle of virtual work referred to a generic element e, with domain Ω_e, may be expressed as (see Belytschko et al. [18]):

$$\int_{\Omega_e} \delta \boldsymbol{u}^T \rho \ddot{\boldsymbol{u}} \, \mathrm{d}\Omega_e + \int_{\Omega_e} \delta \boldsymbol{u}^T \chi \dot{\boldsymbol{u}} \, \mathrm{d}\Omega_e + \int_{\Omega_e} \delta \boldsymbol{\varepsilon}^T \boldsymbol{\sigma} \, \mathrm{d}\Omega_e = \int_{\Omega_e} \delta \boldsymbol{u}^T \boldsymbol{b} \, \mathrm{d}\Omega_e + \int_{\Gamma_e} \delta \boldsymbol{u}^T \bar{\boldsymbol{t}} \, \mathrm{d}\Gamma_e, \tag{1}$$

where ρ is the element's specific mass; χ is the damping coefficient; $\delta \boldsymbol{u}$ is the vector containing the virtual displacements; $\boldsymbol{u}$, $\dot{\boldsymbol{u}}$ and $\ddot{\boldsymbol{u}}$ correspond to displacement, velocity and acceleration vectors, respectively; $\boldsymbol{\sigma}$ is the vector with element stress tensor components; $\delta \boldsymbol{\varepsilon}$ is a vector with components of the virtual strain tensor due to $\delta \boldsymbol{u}$; $\mathbf{b}$ is the body force vector and $\bar{\boldsymbol{t}}$ is the prescribed traction vector applied on Γ_e.

Spatial coordinates, displacements, velocities and accelerations are approximated by the nodal values and the shape functions $\mathbf{N}$ of the eight-node hexahedral finite element. In the FEM context, Eq. (1) leads to the well-known dynamic equilibrium equation expressed in matrix format at element level:

$$\boldsymbol{M}^{(e)} \ddot{\boldsymbol{U}}^{(e)} + \boldsymbol{D}^{(e)} \dot{\boldsymbol{U}}^{(e)} + \boldsymbol{K}^{(e)} \boldsymbol{U}^{(e)} = \boldsymbol{P}^{(e)}, \tag{2}$$

where $\mathbf{M}$, $\mathbf{D}$ and $\mathbf{K}$ are the mass, damping and stiffness matrices, respectively; $\mathbf{P}$ is the external load vector and $\bar{\mathbf{B}}$ is the gradient matrix obtained from the strain-displacement relation $\boldsymbol{\varepsilon} = \bar{\boldsymbol{B}} \boldsymbol{U}$.

2.2 Reduced integration

In the present work, two underintegration techniques for the eight-node hexahedral finite element are employed in order to suppress shear and volumetric locking effects. The first technique utilizes uniform reduced integration, where one-point quadrature is considered for both the deviatoric and volumetric parts of the strain tensor. However, in this case, the so-called hourglass modes may occur and some numerical procedures are necessary to stabilize the element formulation (see Duarte Filho and Awruch [8] for further information). The second technique is the B-bar method proposed by Hughes [19], where only the volumetric part of the strain tensor is underintegrated to avoid volumetric locking.

2.3 Nonlinear analysis with the corotational reference system

A corotational approach is employed here to analyze nonlinear problems. Theoretically, one can decompose the motion of a continuous medium into a rigid body motion followed by a pure deformation portion. Assuming that the finite element discretization is fine enough, the mentioned decomposition at element level can be performed and the pure deformation will be a small amount with respect to the element dimensions. Therefore, the small strain hypothesis can be considered properly. In order to maintain objectivity of the stress updates in the corotational system, stress rate measures are performed in this work using the Truesdell rate tensor. More details on the corotational reference system may be found in Braun and Awruch [9].

In geometrically nonlinear problems, the equilibrium must be iteratively obtained using the incremental approach, where the stiffness matrix and the internal force vector are considered as functions of the current element configuration. In the present work, the Newton-Raphson method is employed and the iterative process continues until the equilibrium is obtained, considering a given tolerance criterion.

For geometrically nonlinear dynamic analysis, the equilibrium equation may be described, in an incremental form, as Mondkar and Powell [20]:

$$\boldsymbol{M}\Delta\ddot{\boldsymbol{U}} + \boldsymbol{D}\Delta\dot{\boldsymbol{U}} + \boldsymbol{K}_t\Delta\boldsymbol{U} = \boldsymbol{P}_{t+\Delta t} - \left[\boldsymbol{f}^{\text{int}}(\boldsymbol{U}) + \boldsymbol{M}\ddot{\boldsymbol{U}} + \boldsymbol{D}\dot{\boldsymbol{U}}\right]_t, \tag{3}$$

where **M**, **D** and **K** are the mass, damping and stiffness matrices, respectively; $\Delta\ddot{\mathbf{U}}$, $\Delta\dot{\mathbf{U}}$ and $\Delta\mathbf{U}$ are, respectively, vectors containing incremental values of acceleration, velocity and displacement; $\mathbf{K}_t$ is the tangent stiffness matrix at time t and $\mathbf{P}_{t+\Delta t}$ is the load vector at time $t+\Delta t$. Note that inertial and dumping forces vanishes for static analysis and the previous equation is simplified.

In the present work, the Newmark's method and the Generalized-α method are applied in the previous equation for time integration (see Duarte Filho and Awruch [8] and Braun and Awruch [9] for further information).

As with the geometric nonlinear analysis, a corotational system is also used at element level for the integration of elastoplastic constitutive equations. The numerical integration scheme for updating stress states adopted in the present study is based on the algorithm presented by Owen and Hinton [21].

3 Contact formulation

3.1 Contact kinematics

Consider two bodies (α = 1,2) about to get in touch, where $\overline{\mathbf{x}}^1$ is the vector containing the coordinates of the orthogonal projection on the master surface of the slave node with coordinates $\mathbf{x}^2$.

The non-penetrability condition, using the closest point projection method, is defined as:

$$g_N = (\mathbf{x}^2 - \overline{\mathbf{x}}^1)\cdot\overline{\mathbf{n}}^1 \geq 0, \tag{4}$$

where the outward unit normal vector $\overline{\mathbf{n}}^1$ is obtained using the cross product between the tangent vectors $\overline{\mathbf{a}}_1^1$ and $\overline{\mathbf{a}}_2^1$. The tangent vectors are defined in a local convective coordinate system using parametric coordinates $\overline{\boldsymbol{\xi}}^\beta$, i.e. $\overline{\mathbf{a}}_\beta^1 = \overline{\mathbf{x}}_{,\beta}^1(\overline{\boldsymbol{\xi}}^\beta)$ (β = 1,2).

The first step in the calculation of normal gap between bodies is called "global search" and consists of finding which target elements are candidates to get in touch with the slave node. After that, a "local search" is carried out to evaluate the slave node projection on the target surface ($\overline{\mathbf{x}}^1$) using an iterative process. If the contact is not detected, a new search is performed for other contact candidates.

In the tangential direction two cases are considered: stick and sliding. In the stick case, the slave node is not allowed to move in a tangential direction on the master surface and, therefore, the convective coordinates $\overline{\boldsymbol{\xi}}^\beta$ do not change during motion, while in the sliding case the slave node is allowed to move in a tangential direction on the contact surface (see Wriggers [16] and Laursen [17] for more details).

3.2 Contact contribution to the weak form

The penalty method is employed here for the treatment of contact problems, where terms are added to the traditional virtual work principle, Eq. (1), which correspond to the virtual work done by the contact tractions $\boldsymbol{t}$ related to the virtual displacement field $\delta\boldsymbol{g}$ on the contact boundary Γ_c (see Wriggers [16]):

$$\int_{\Omega_e}\delta\boldsymbol{u}^T\rho\ddot{\boldsymbol{u}}\,\mathrm{d}\Omega_\mathrm{e} + \int_{\Omega_e}\delta\boldsymbol{u}^T\chi\dot{\boldsymbol{u}}\,\mathrm{d}\Omega_\mathrm{e} + \int_{\Omega_e}\delta\boldsymbol{\varepsilon}^T\boldsymbol{\sigma}\,\mathrm{d}\Omega_\mathrm{e} = \int_{\Omega_e}\delta\boldsymbol{u}^T\boldsymbol{b}\,\mathrm{d}\Omega_\mathrm{e} + \int_{\Gamma_e}\delta\boldsymbol{u}^T\overline{\boldsymbol{t}}\,\mathrm{d}\Gamma_\mathrm{e} + \int_{\Gamma_c}\delta\boldsymbol{g}^T\boldsymbol{t}\,\mathrm{d}\Gamma_c. \tag{5}$$

The previous system of nonlinear equations is solved here using the Newton-Raphson method, where linearization procedures must be carried out considering an incremental-iterative approach. In this case, a contact stiffness matrix is obtained. A detailed description on linearization of the contact virtual work may be found in

Wriggers [16] and Laursen [17].

4 Numerical example

The present example seeks to evaluate the interaction between a shallow foundation resting on a three-dimensional soil layer where the structure is under a cyclic load with geometrical characteristics shown in Fig. 1a.

Due to symmetry, only half of the problem is modeled with 1948 8-node hexahedral elements and 2561 nodes (Fig. 1b). A rough frictional contact between the soil-structure interface was assumed and, therefore, the interface elements can open a gap but no sliding is allowed. The normal and tangential penalty parameter employed here are equal to 4.0 x 10^3 kN/m.

The soil was modeled with Drucker-Prager yield criterion assuming coincidence at the outer edges with the Mohr-Coulomb surface, while the structure is considered as an elastic material (Table 1). It is possible to notice that the Young's modulus for the soil is a function of the initial confining pressure (σ_3 in kN/m²) which is evaluated at the center of the finite element using the soil specific weight equal to 16 kN/m².

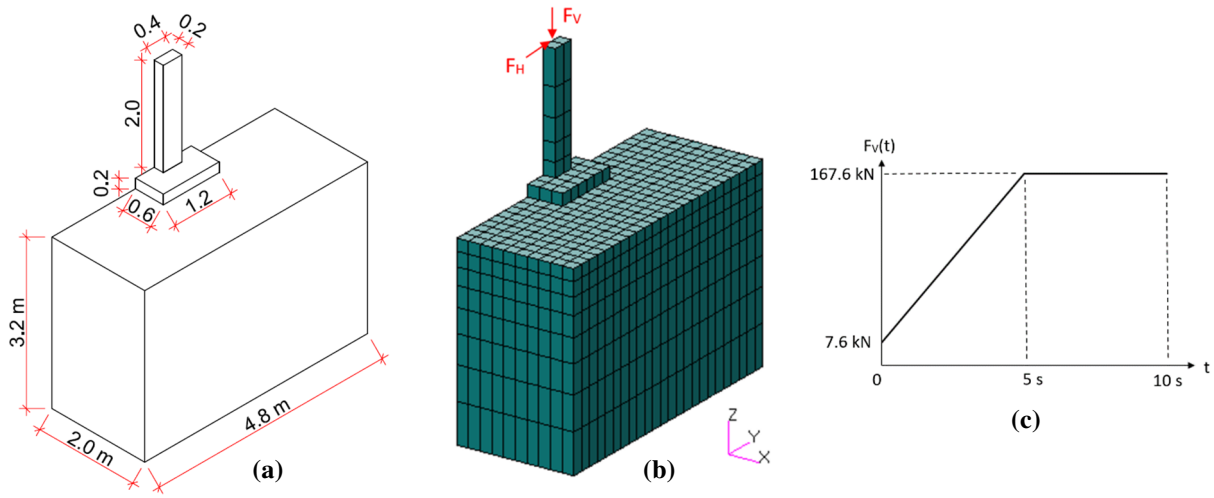

Figure 1. (a) Geometrical characteristics, (b) initial mesh configuration and (c) load description

Table 1. Physical parameters adopted for the soil-structure interaction problem

Soil	Young's modulus – E	40000 x $(\sigma_3/100)^{0.86}$ kN/m²
	Poisson's ratio – ν	0.33
	Angle of friction – ϕ	42°
	Cohesion – c	1.2 kN/m²
	Specific mass - ρ	1.631 x 10^3 kg/m³
Structure	Young's modulus – E	30 x 10^6 kN/m²
	Poisson's ratio – ν	0.20
	Specific mass - ρ	2.548 x 10^3 kg/m³

Nodes located on the base of the computational domain are fixed in all directions while the lateral walls are constrained against movement only in the horizontal plane, just as the structure nodes that are on the symmetry plane. In the static analysis, a compressive axial load of 160 kN and a horizontal load of 2 kN are applied at the column free end with 200 load steps and a compressive axial load of 7.6 kN is fully applied at the beginning of the simulation to reproduce the structure self weight. The dynamic analysis is performed during 10 s with Δt = 5.0 x 10^{-3} s, where the axial load description is shown in Fig. 1c and the horizontal load is defined as a sinusoidal function with the same amplitude defined in the static analysis, i.e.: $F_H = 2.0\sin(2\pi t)$ kN.

Two points are used to measure the displacements: point A, corresponding to the point where the loads are applied and point B, which corresponds to a point on the soil-structure interface and located at a central point

underneath the footing, in the symmetry axis.

Results computed here are compared with those obtained using the finite element commercial software ANSYS. The soil was modeled using SOLID65 elements, which support the classic Drucker-Prager model, and the structure was modeled using SOLID185 elements. Both elements are defined by eight nodes having three degrees of freedom at each node.

In the static analysis, the vertical and horizontal displacements observed at point A were, respectively, -5.30 cm and 7.82 cm for the element with one-point quadrature, -5.02 cm and 5.60 cm for the element with B-bar formulation and -4.62 cm and 3.72 cm for the ANSYS results. It is possible to notice that values obtained for the element with one-point quadrature were larger than the other results, once the entire element loses stiffness when the yield stress is reached.

Load-displacements curves evaluated at point B are plotted in Figs. 2 and 3, while the horizontal displacements evaluated at point A are shown in Fig. 4. It is important to mention that ANSYS did not converge using the Newmark's method and it was necessary to use the Generalized HHT-α method, where a numerical dissipation is introduced, similar to the Generalized-α method adopted in the present algorithm.

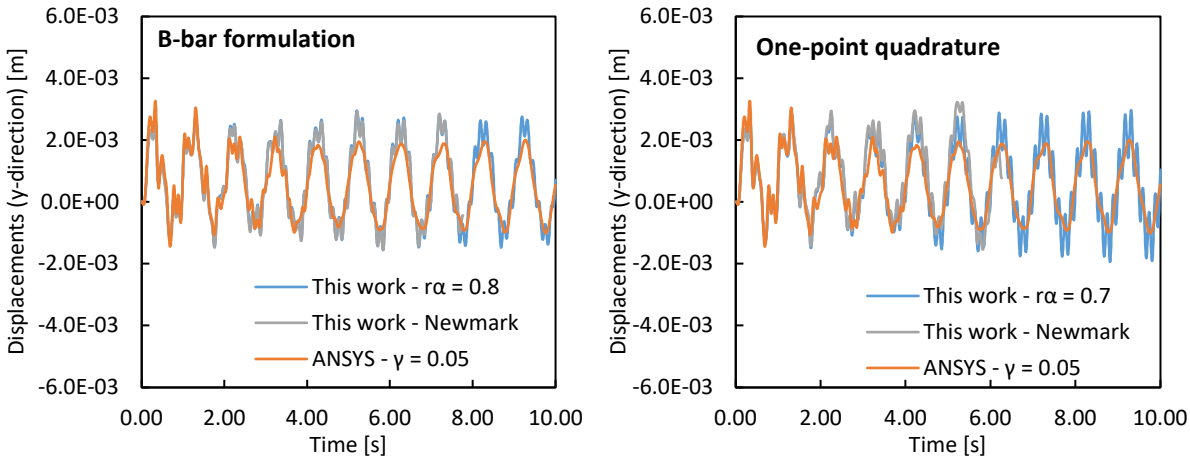

Figure 2. Horizontal displacement response at point B for the soil-structure problem

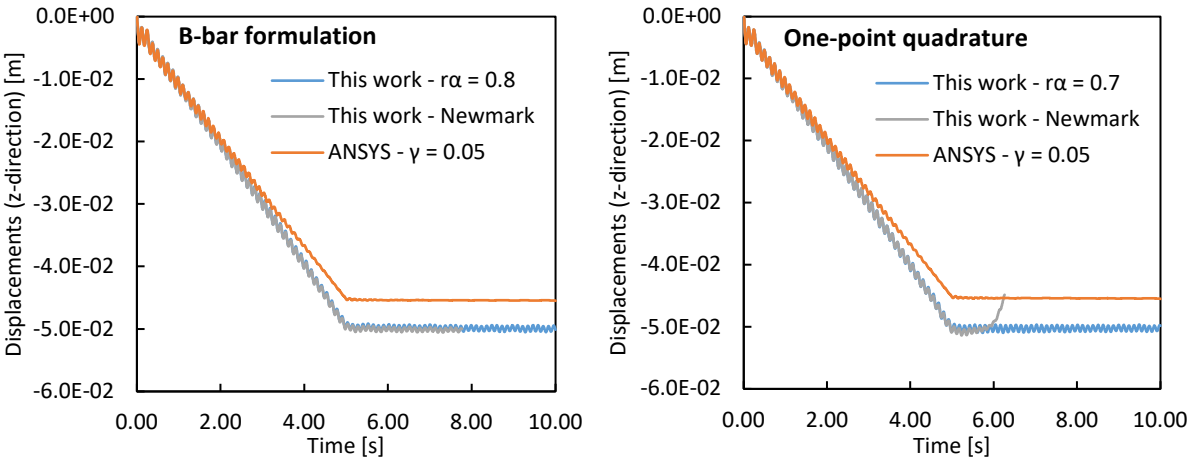

Figure 3. Vertical displacement response at point B for the soil-structure problem

It is observed in Figs. 2, 3 and 4 that the Newmark's method was unable to complete the analysis and, therefore, it was necessary to employ the Generalized-α method to stabilize the time integration process with r_α = 0.8 for the analysis with B-bar formulation and r_α = 0.7 for the analysis with one-point quadrature. It is observed that results obtained with ANSYS were similar to those measured in the present work with a small divergence after 5 s. One can see that the ANSYS formulation showed a large amount of numerical dissipation, which

strongly dissipates vertical displacement oscillations, especially after $t = 4$ s.

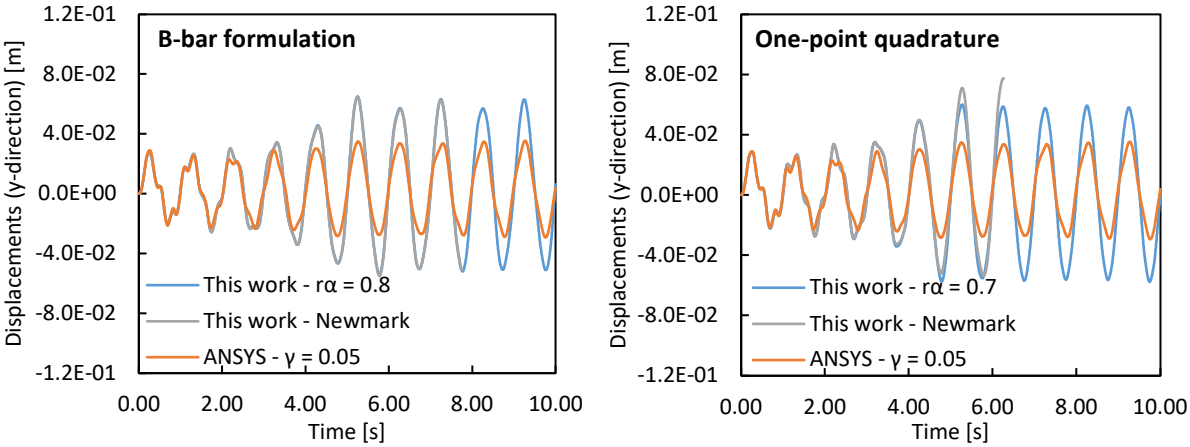

Figure 4. Horizontal displacement response at point A for the soil-structure problem

In order to evaluate the structure response resting on a rigid base, two other models were performed: a model with structure in contact with a rigid surface and a model where structure base nodes fixed in all directions. Dynamic analysis is performed using the B-bar formulation and the Newmark's method. The displacements measured at point A for both models are presented in Fig. 5, where it is possible to notice that all models are in agreement with each other. Note that the horizontal displacements values obtained in these models were very small compared to those where the soil was simulated. The maximum values obtained for the structure resting on a rigid base were at least 200 times smaller than those obtained with ANSYS' soil-structure model.

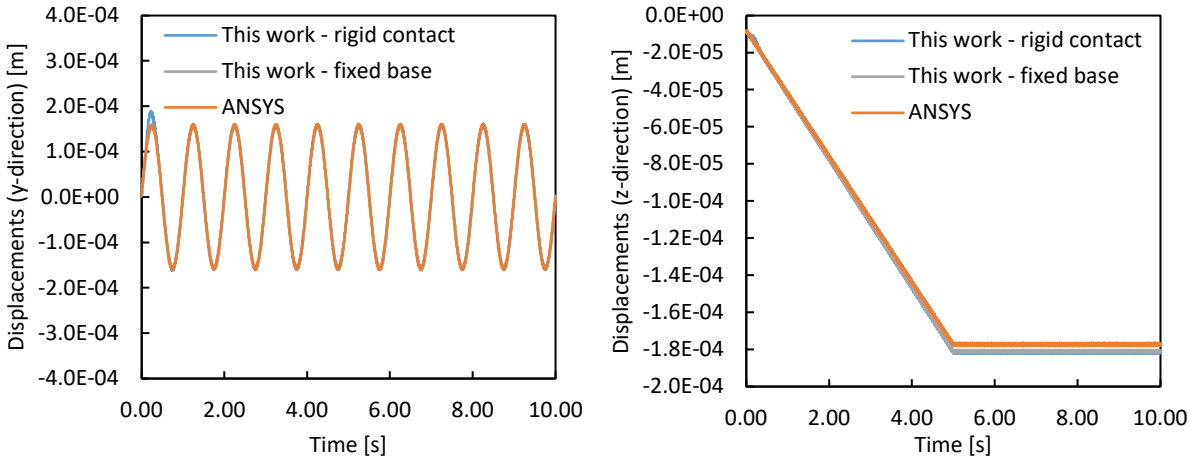

Figure 5. Displacement response at point A for the structure resting on a rigid base

5 Conclusions

A numerical example of a shallow foundation resting on a three-dimensional soil layer where the structure is under a cyclic load was performed in the present work in order to obtain the soil influence on the dynamic response. Spatial discretization of the bodies in contact was carried out by employing the Finite Element Method (FEM) and eight-node hexahedral isoparametric elements with two underintegration methods. It was observed that the Newmark's method was not able to complete the non-linear elastodynamic analysis and, therefore, it was necessary to employ the Generalized-α method with appropriate spectral radius. Results obtained with both underintegration methods were very similar between each other and despite ANSYS solution showed a large amount of numerical dissipation, in general, numerical results presented a good agreement with a few differences. It was also shown that the dynamic response of the structure resting on a flexible soil showed a very

different behavior when compared to the same structure resting on a rigid base. Although results concerning the numerical efficiency of element formulation were not showed in this work, simulations indicated that using hexahedral elements with one-point quadrature led to a shorter processing time, which is a very important feature for nonlinear problems such as contact applications. The present algorithm is still being implemented and other numerical examples will be used to fully validate it.

Acknowledgements. The authors would like to thank to Capes and CNPq for the financial support.

Authorship statement. The authors hereby confirm that they are the sole liable persons responsible for the authorship of this work, and that all material that has been herein included as part of the present paper is either the property (and authorship) of the authors, or has the permission of the owners to be included here.

References

[1] A. K. Chopra and J. A. Gutierrez, "Earthquake response analysis of multistorey buildings including foundation interaction". *Earthquake Engineering & Structural Dynamics*, vol. 3, n. 1, pp. 65-77, 1974.
[2] J. Bielak, "Modal analysis for building-soil interaction". *Journal of the Engineering Mechanics Division*, vol. 102, n. 5, pp. 771-786, 1976.
[3] M. Novak and L. E. Hifnawy, "Damping of structures due to soil-structure interaction". *Journal of Wind Engineering and Industrial Aerodynamics*, vol. 11, n. 1-3, pp. 295-306, 1983.
[4] L. Menglin et al., "Structure–soil–structure interaction: Literature review". *Soil Dynamics and Earthquake Engineering*, vol. 31, n. 12, pp. 1724-1731, 2011.
[5] S. C. Dutta and R. Roy, "A critical review on idealization and modeling for interaction among soil–foundation–structure system". *Computers & structures*, vol. 80, n. 20-21, pp. 1579-1594, 2002.
[6] E. Kausel, "Early history of soil–structure interaction". *Soil Dynamics and Earthquake Engineering*, vol. 30, n. 9, pp. 822-832, 2010.
[7] Y. K. Hu and L. I. Nagy, "A one-point quadrature eight-node brick element with hourglass control". *Computers & structures*, vol. 65, n. 6, pp. 893-902, 1997.
[8] L. A. Duarte Filho and A. M. Awruch, "Geometrically nonlinear static and dynamic analysis of shells and plates using the eight-node hexahedral element with one-point quadrature". *Finite Elements in Analysis and Design*, vol. 40:1, pp. 1297-1315, 2004.
[9] A. L. Braun and A. M. Awruch, "Geometrically non-linear analysis in elastodynamics using the eight-node finite element with one-point quadrature and the generalized-α method". *Latin American Journal of Solids and Structures*, vol. 5, n. 1, pp. 17-45, 2008.
[10] D. Schmidt. Análise elastoplástica com não-linearidade geométrica de estruturas através de elementos hexaédricos tri-lineares com um ponto de integração. MSc thesis (in Portuguese), Universidade Federal do Rio Grande do Sul, 2006.
[11] S. Reese, "On a physically stabilized one point finite element formulation for three-dimensional finite elasto-plasticity". *Computer Methods in Applied Mechanics and Engineering*, vol. 194, n. 45-47, pp. 4685-4715, 2005.
[12] A. L. Braun and A. M. Awruch, "An Efficient Model for Numerical Simulation of the Mechanical Behavior of Soils: Part 1: Theory and Numerical Algorithm". *Soils and Rocks*, vol. 36, n. 2, pp. 159-169, 2013.
[13] A. L. Braun and A. M. Awruch, "An Efficient Model for Numerical Simulation of the Mechanical Behavior of Soils: Part 2: Applications". *Soils and Rocks*, vol. 36, n. 2, pp. 171-182, 2013.
[14] T. A. Laursen and J. C. Simo. "A continuum-based finite element formulation for the implicit solution of multibody, large deformation-frictional contact problems". *International Journal for numerical methods in engineering*, vol. 36, n. 20 pp. 3451-3485, 1993.
[15] X. Chen et al., "Finite element analysis for large deformation frictional contact problems with finite sliding". *JSME International Journal*, series A, vol. 42, n. 2, pp. 201-208, 1999.
[16] P. Wriggers. *Computational contact mechanics*. Springer, 2nd ed., 2006.
[17] T. Laursen. *Computational contact and impact mechanics*: fundamentals of modeling interfacial phenomena in nonlinear finite element analysis. Springer, 2003.
[18] T. Belytschko et al. *Nonlinear finite elements for continua and structures*. John Willey & Sons, 2nd ed., 2014.
[19] T. J. Hughes, "Generalization of selective integration procedures to anisotropic and nonlinear media". *International Journal for Numerical Methods in Engineering*, vol. 15, n. 9, pp. 1413-1418, 1980.
[20] D. P Mondkar and G. H. Powell, "Finite element analysis of non-linear static and dynamic response". *International journal for numerical methods in engineering*, vol. 11, n. 3, pp. 499-520, 1977.
[21] D. R. J. Owen and H. Hinton. *Finite elements in plasticity*: Theory and Practice. Pineridge Press, 1980.